Hindawi
International Journal of Antennas and Propagation
Volume 2024, Article ID 6659390, 14 pages
https://doi.org/10.1155/2024/6659390

Research Article

Design and Realization of an *X* Band Monopulse Feed Antenna for Low Earth Orbit (LEO) Satellite Ground Station

İsmail Şişman,[1,2] **Tugba Haykir Ergin**,[2] **Duygun Erol Barkana**,[2] **and Hüseyin Arda Ülkü**[2]

[1]*Research and Development Department, Profen Communication Technologies, Istanbul, Türkiye*
[2]*Department of Electrical and Electronics Engineering, Yeditepe University, Istanbul, Türkiye*

Correspondence should be addressed to İsmail Şişman; ismail.sisman@profen.com

Received 27 May 2023; Revised 28 January 2024; Accepted 31 January 2024; Published 26 February 2024

Academic Editor: Giovanni Andrea Casula

In this work, design of a five-element compact dual-polarization *X* band monopulse feed antenna using a 7.3 m Cassegrain-type reflector for Low Earth Orbit (LEO) satellite ground station is presented. The designed antenna has reached 32 dB/K G/T value, the side lobe level of the designed antenna is at the level of −24 dB, the crosspolarization value is −35 dB, and the port isolation value is below −29 dB in the 8–8.5 GHz frequency range. The antenna efficiency of the designed antenna is measured as 79.93%.

1. Introduction

Low Earth Orbit (LEO) or remote sensing satellites move faster relative to ground stations. Therefore, tracking fast-moving earth observation LEO satellites precisely is essential to get image data without interruption. In such cases, the efficiency of the tracking system highly depends on the feed of the antenna system; hence, the feed architecture is important for an effective tracking system [1].

In the literature, sequential lobing, conical scan, and monopulse tracking are well-known target tracking techniques [2]. Among these techniques, monopulse tracking has shown to have a high signal-to-noise ratio (SNR), is mechanically vibration-free [3], and provides high-precision tracking [4]. For example, the trajectory of an LEO satellite has been estimated precisely using orbital Keplerian characteristics in the program tracking approach in [5].

Monopulse tracking systems use multiple antennas to gather angular data in the azimuth and elevation axes with different configurations; e.g., four-elements [6, 7], five-elements [8, 9], and multimode feed [10] have been used depending on the application, system specification, and cost-effectiveness. Monopulse feed is the most commonly used and effective tracking technique [4]. The feed design provides an accurate tracking system with the optimum sum and difference patterns for high gain and low beam width reflectors [11]. Various research studies for the single-band operation have been made to find the best feed for monopulse tracking [12]. Monopulse feeds have been shown to demonstrate a dual-polarized tracking element for a five-element feed [13]. The total signal is extracted from a conical or corrugated horn antenna with a larger aperture in a setup with five horn antennas. The error signal in the azimuth and elevation axes is retrieved from a smaller waveguide with a circular aperture. Modern satellites use polarization diversity to concurrently transmit information in two channels of the same frequency to support a higher data rate within the constrained bandwidth available. Right-hand circular polarization (RHCP) and left-hand circular polarization (LHCP) signals are concurrently delivered by LEO satellites operating in circular polarization under frequency reuse systems. Therefore, tracking the LEO satellites using both polarization techniques to collect error-free satellite data is crucial [14].

This study focuses on designing and implementing a combined single-band with dual-polarization monopulse feed at 8–8.5 GHz with a high efficiency of 79.93% and a high gain to construct a high-precision tracking system. The

proposed feed is ideal for X single-band operation, which is small, straightforward, and simple. The proposed X band feed antenna consists of a septum polarizer, a corrugated horn antenna, and a monopulse unit. The proposed X band feed antenna is constructed using a 7.3 m Cassegrain-type reflector. The CST Studio Suite [15] software is used to design, model, and analyze the proposed antenna. The performance outputs of the designed antenna match the design criteria and are compared with the similar designs in the literature.

In the proposed design, the crosspolarization isolation value is above 35 dB, the side lobe level exceeds 24 dB, and the antenna directivity is 54.97 dBi resulting in superior performance. This directly influences the system G/T value. The monopulse tracking block diagram in this study differs from conventional monopulse tracking systems [7]. In the presented structure, the TE11 mode from both azimuth and elevation is initially combined and then fed into a 180° hybrid coupler and subsequently into a 90° hybrid coupler. This configuration allows the system to track in both RHCP and LHCP, creating a versatile tracking system.

The rest of the paper is designed as follows: in Section 2, the design of each component of the X band feed antenna, i.e., septum polarizer, corrugated horn antenna, and monopulse unit, and their assemblies are presented. In Section 3, the assembly of the reflector antenna and the designed feed antenna is explained. In Section 4, measurement results are presented, and conclusions are drawn in Section 5.

2. Design of X Band Feed Antenna

The X band feed antenna system comprises a septum polarizer, a corrugated horn antenna, and a monopulse feed unit as shown in Figure 1. These components must be designed for the feed antenna to successfully receive the communication and tracking signal and to maintain the system's continuity. Each component must provide the required RF characteristics individually, and when all components are assembled, the RF characteristics of the system must also be maintained. The targeted system performance specifications of the proposed X band feed antenna system for the LEO ground station are given in Table 1. While designing components in this section, the wavelength λ at the 8.25 GHz is used. In this study, an X band septum polarizer is selected for the polarization conversion of the signal received by the feed antenna, the X band feed antenna is selected as a corrugated horn antenna, and a monopulse unit is used to calculate the difference between the satellite and the ground station boresight from the signal received by the antenna during satellite communication.

The X band feed system is evaluated on the 7.3 m Cassegrain reflector. In this study, a Cassegrain antenna structure is used in the X band feeding system because a Cassegrain antenna has less obstruction in front of the reflector when using two reflectors than a single reflector. In the Cassegrain structure, the X band feed antenna is placed in the virtual focus between the primary and second reflectors. The feed antenna provides the receiving part of the communication signal in the X band feed antenna.

Next, the design of each component and their assembly are explained in detail.

2.1. Septum Polarizer Design. The primary purpose of the design is to linearly transmit half of the power of the RHCP or LHCP wave from the square waveguide to one of the two rectangular waveguides depending on the polarization characteristics. While achieving this goal, it is necessary to keep reflection values at the inputs and outputs of the structure and the isolation value between the rectangular waveguides low.

The design of a septum polarizer consists of three parts: the square waveguide, the septum step structure, i.e., a segment consisting of several steps, and two rectangular waveguides, i.e., the parts at the end of the septum where linear signals are received. The square waveguide dimensions are calculated depending on the frequency band. For a rectangular waveguide, the sizes are calculated as follows:

$$f_{c_{m,n}} = \frac{1}{2\pi\sqrt{\mu\epsilon}}\sqrt{\frac{m\pi^2}{a} + \frac{n\pi^2}{b}}, \tag{1}$$

where $f_{c_{m,n}}$ represents the cutoff frequency of the (m, n) mode and (a, b) indicates the dimensions of the waveguide.

The square waveguide size for 8–8.5 GHz is calculated as $a = b = 24$ mm, and the size of the waveguide structure is shown in Figure 2(a).

In the septum polarizer design, a 4-step septum structure is used. Additionally, a conductive tooth is designed near the square waveguide for impedance matching. The dimensions of the septum steps are designed depending on the wavelength. The lengths of the septum step structure are shown in letters in Figure 2(b), and the dimensions of the steps are shown in millimeters in Figure 2(c).

Finally, the parts where linear signals are received at the end of the septum polarizers are designed. These parts can be designed with a waveguide or a pin structure. In this study, WR112 rectangular waveguides are used for the design. At the end of the septum, waveguides are rotated 90° and designed as two waveguides on the right and left sides. The appearance of the structure is given in Figure 2(d).

Aluminum is used as the material for the design and fabrication of the septum polarizer. The common port is called port 3, and it is expected as the input port for a circularly polarized wave; then, the LHCP signal is received from port 1 (left port in Figure 2(d)), and the RHCP signal is received from port 2 (right port in Figure 2(d)).

If a common port is used as input, then two signals are generated: parallel and perpendicular to the septum plane and summed. Thus, the phase difference between these signals is 90°.

Theoretically, half of the signal sent from the common port is expected to reach one of the linear ports, corresponding to −3 dB and a 90° phase difference between them.

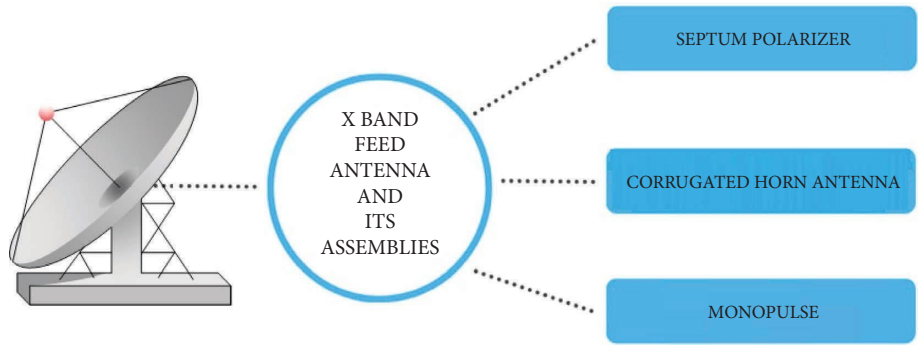

Figure 1: The schema of the structural design of X band feed antenna.

Table 1: Target specifications of the X band feed antenna with 7.3 m Cassegrain-type reflector.

Parameters	Specifications
Gain	54.80 dBi @8250 MHz
Voltage standing wave ratio (VSWR)	1 : 1.2
Crosspolarization	−30 dB
Null depth	30 dB
Port isolation	−28 dB
Side lobe level (SLL)	−18 dB
G/T @8250 MHz	32 dB/K

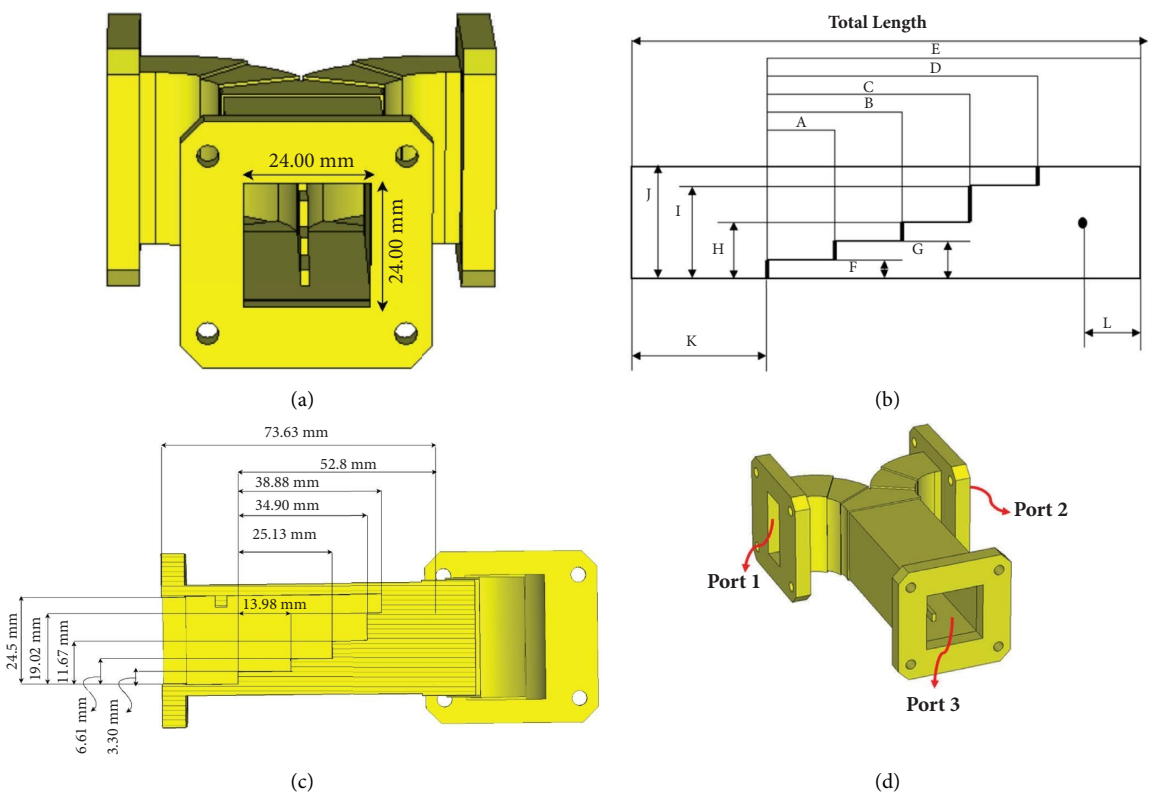

Figure 2: The septum polarizer: (a) the front view, (b) the septum step structure and length parameters, (c) the septum step dimensions, and (d) the position of the waveguide in the septum polarizer.

2.2. Corrugated Horn Antenna Design. The feed antenna is the interstage system that receives the electromagnetic wave from the air and transfers it to the transmission line. In this study, the X band feed antenna is chosen as a corrugated horn antenna as shown in Figure 3. Three critical are taken into consideration in the design of the feed antenna: antenna beamwidth, illumination angle phase variation, and feed antenna-air matching. Corrugations are added after the input radius of the structure is

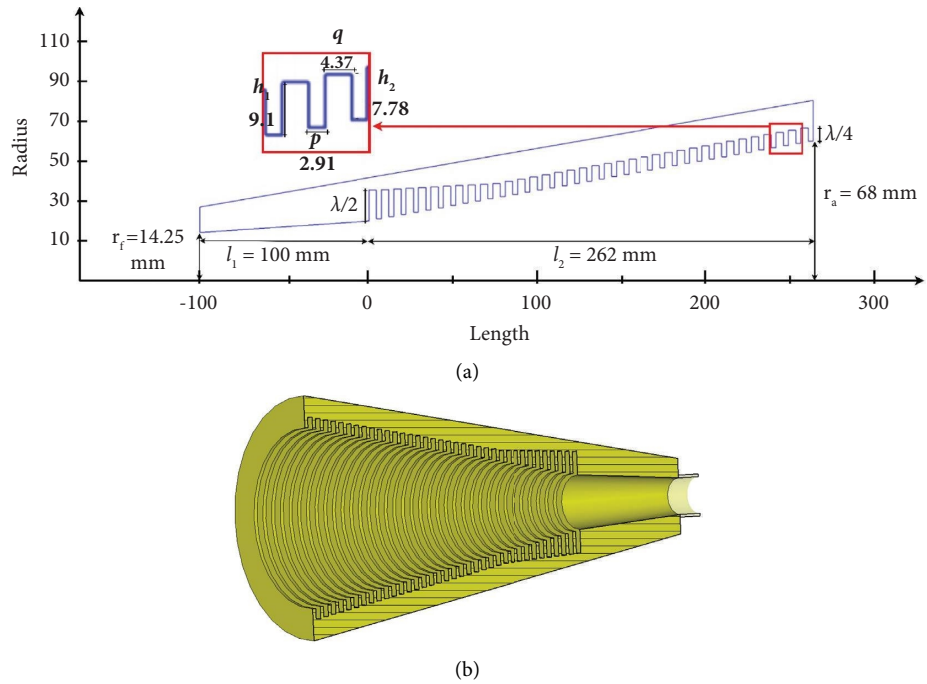

Figure 3: Corrugated horn antenna as feed antenna: (a) dimensions and (b) mechanical structure profile.

calculated. The depth of the first corrugation placed at the entrance of the antenna is $\lambda/2$, and the depth of the subsequent corrugations is gradually reduced from $\lambda/2$ to $\lambda/4$ with a total of 10 corrugations. This section consisting of 10 corrugations with decreasing dimensions is called the mode converter. The depth of the rest of the corrugations in the body of the antenna is equal to $\lambda/4$, and the number of corrugations used in the body is given parametrically with the width and tooth thickness of the corrugations in the CST Studio Suite [15] software, which optimizes the structure by changing the parameter values. The resulting schematic and dimensions of the designed corrugated system after the optimization are shown in Figure 3(a). The designed corrugated structure shown in Figure 3(a) is rotated 360° in the waveguide axis, and the mechanical structure is obtained. A cross-sectional view of the mechanical structure of the feed antenna is given in Figure 3(b).

2.3. Monopulse Unit Design. The tracking system is realized by the monopulse unit, which consists of four circular waveguides placed two by two in azimuth and elevation of the feed antenna as shown in Figure 4. The number, position, and dimensions of the waveguides used in the monopulse unit are calculated precisely for the design.

Initially, the signal modes are analyzed to calculate the size of the waveguides [16]. The input of the feed antenna is designed as a circular waveguide since the signal received by the antennas is a circularly polarized wave. The feed antenna must receive the communication mode of the signal. The communication mode corresponds to TE11 among the circular waveguide modes. The X band feed antenna is required to operate in the 8–8.5 GHz frequency band. The cutoff frequency must be lower than the minimum frequency value so that the structure can operate efficiently after 8 GHz. The cutoff frequency chosen for this design is 7 GHz. The circular waveguide's input radius is 12.56 mm. As a result of the simulations, the optimum radius value is 14.25 mm.

Designing an accurate tracking system with optimum sum and difference patterns for a high gain narrow beamwidth reflector is mainly based on the feed design. The monopulse section is added to the structure after the feed antenna design. The monopulse section samples the signal from the feed antenna. Thus, the dimensions of the circular waveguides in the monopulse unit are designed as 14.25 mm. Data in elevation and azimuth are required to calculate the error signal by sampling the signal to the antenna. Therefore, four monopulse couplers are designed to receive data from the circularly polarized signal in each axis. These couplers are placed two each in azimuth and elevation of the feed antenna. The five-element structure consisting of a corrugated antenna and four circular waveguides is shown in Figure 4. A block diagram of the monopulse tracking system is given in Figure 5. The system can perform monopulse tracking for both RHCP and LHCP without the knowledge of the polarization type of the satellite to be tracked. A quadrature tracking system separates the feed antenna for elevation (E) and azimuth (A) axes.

In this system, septum polarizers are installed at the rear part of the waveguide structure to generate RHCP and LHCP polarizations in the tracking error signal. The output signals of $E1$ and $E2$ waveguides along the elevation axis are first combined using a 2-way power combiner. Similarly, the output signals of $A1$ and $A2$ waveguides along the azimuth axis are combined using a 2-way power combiner. As a result, the signals are connected to a 180-degree hybrid coupler, creating an elevation error signal with RHCP polarization for tracking.

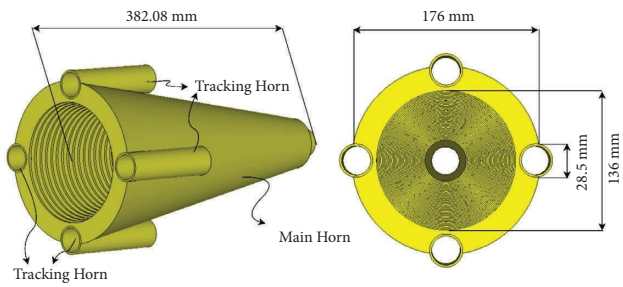

Figure 4: Three-dimensional view and front view of the feed and tracking antenna.

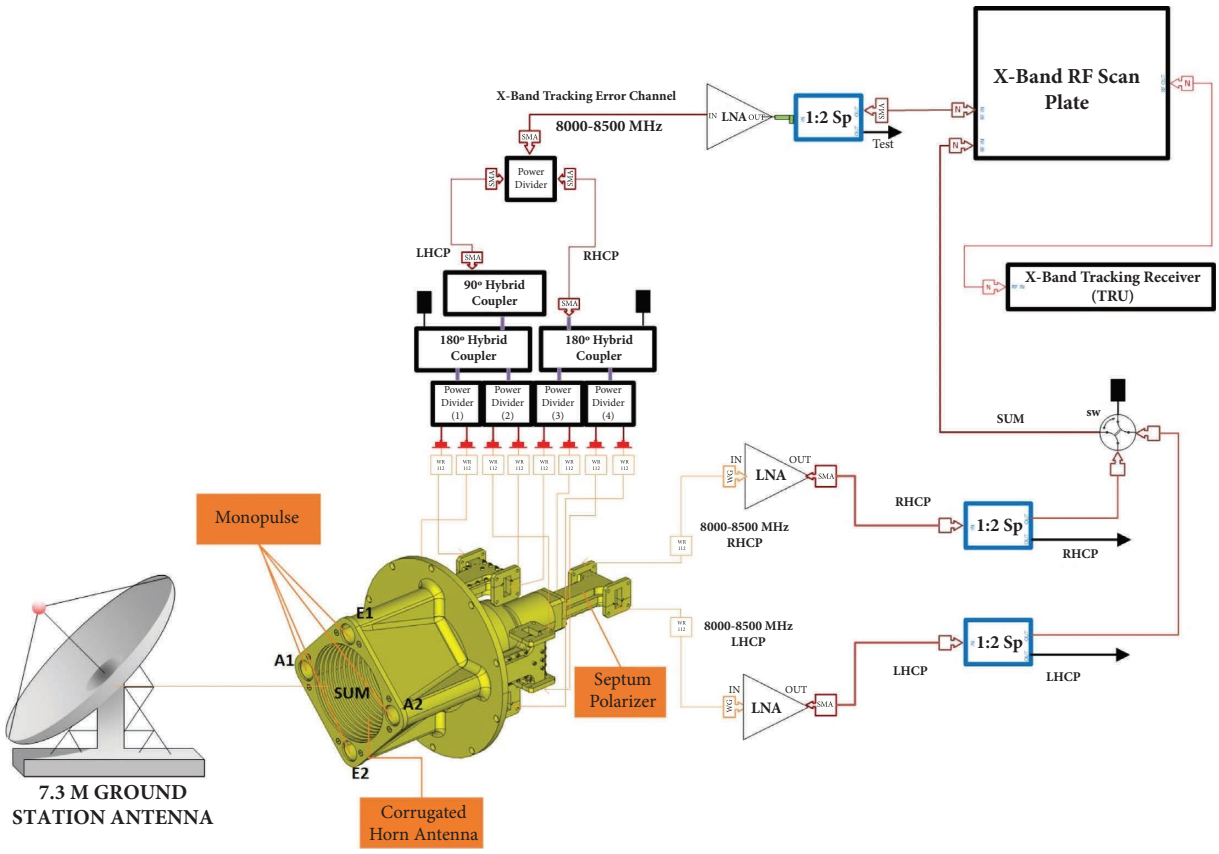

Figure 5: Monopulse tracking block diagram.

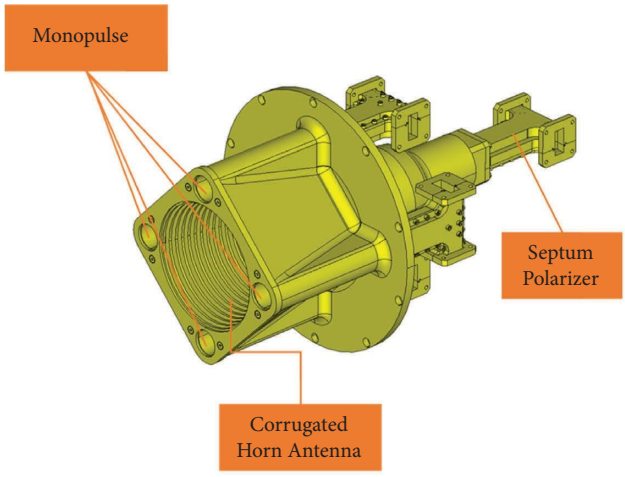

Figure 6: X band feed antenna.

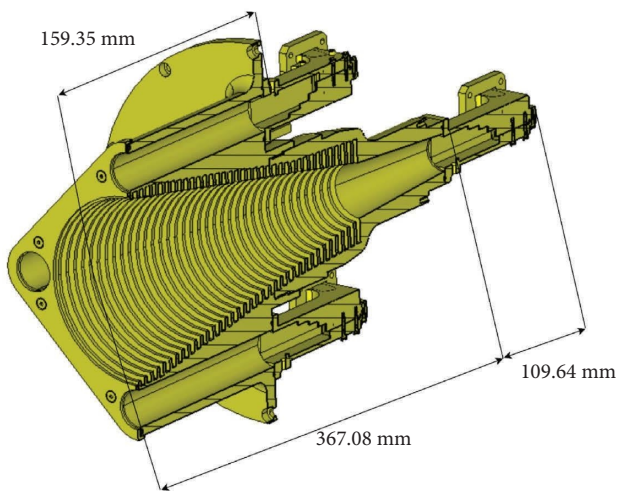

Figure 7: Dimensions of feed antenna and its assemblies.

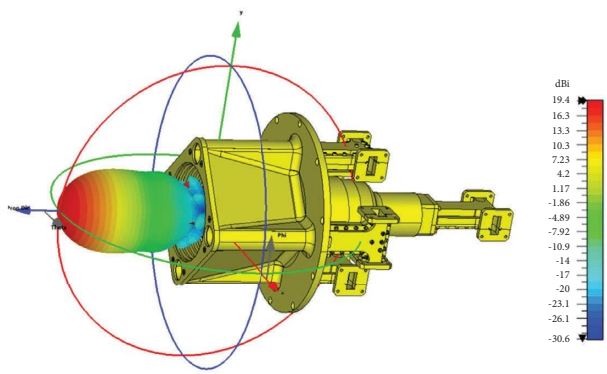

Figure 8: The radiation pattern of the X band feed antenna system at 8.25 GHz.

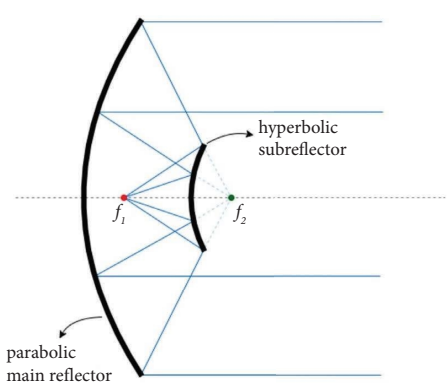

Figure 9: The structure of the Cassegrain antenna structure.

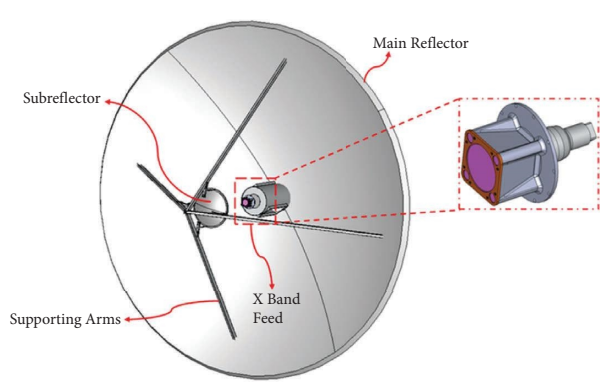

Figure 10: The feed antenna position on the 7.3 m Cassegrain reflector.

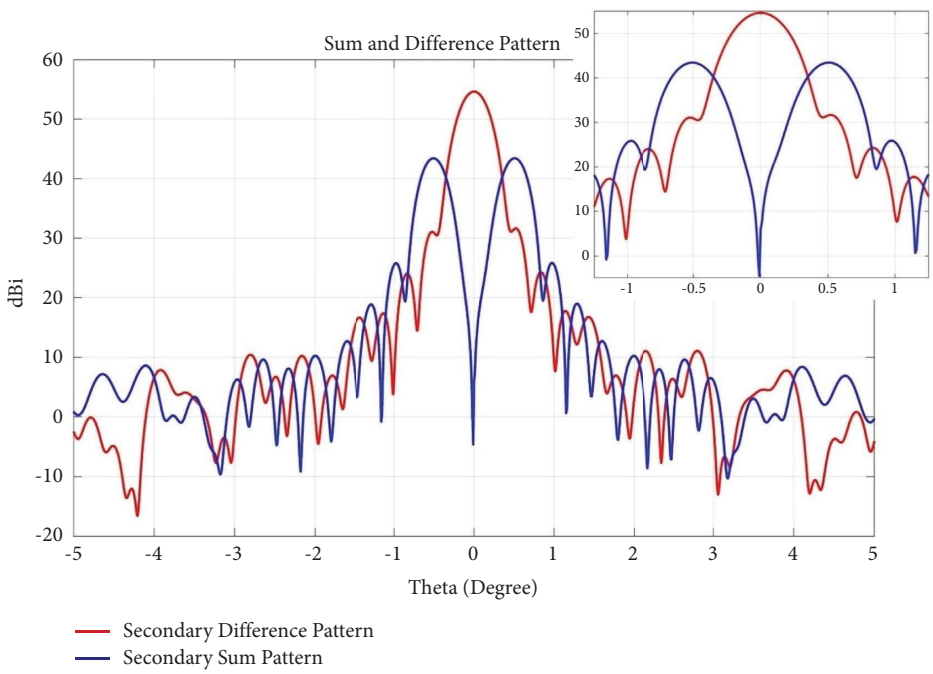

Figure 11: Secondary sum and difference pattern plot for 7.3 m Cassegrain antenna.

Likewise, the output signals of $A1$ and $A2$ waveguides along the azimuth axis are combined using a 2- way power combiner, and then the output signals of $A1$ and $A2$ waveguides are combined using another 2-way power combiner. This creates signals connected to a 180-degree hybrid coupler and then to a 90-degree hybrid coupler, generating an azimuth error signal with LHCP polarization for tracking.

Both elevation and azimuth error signals, being in phase, are combined using a power combiner to create the tracking error signal. This signal passes through a low-noise amplifier and is then sent to an X band RF scan plate. The sum signal at the septum polarizer output has the characteristics of RHCP and LHCP circular polarizations, and a low-noise amplifier amplifies each polarization line and then switches. Switching is done based on the tracked satellite's polarization, and the sum signal is sent to the X band RF scan plate.

The RF scanning plate consists of an isolator, power combiner, variable attenuator, phase shifter, and frequency down-converter. The azimuth and elevation information generated from the difference and sum signals of the antenna is sent to the automatic tracking receiver to enable the antenna to track the satellite signal.

2.4. Assembly of Septum Polarizer, Corrugated Horn Antenna, and Monopulse. The septum polarizer, corrugated horn antenna, and monopulse unit are combined and simulated. The design is shown in Figure 6.

Ten ports are defined on the structure. Two of these ports are the ports that will receive the circularly polarized communication signal. Four ports are the ports of the circular waveguides on the elevation axis for the tracking signal; the other four ports are the ports of the circular waveguides on the azimuth axis for the tracking signal.

After the design of the feed antenna, four circular waveguides, called monopulse units, are added in azimuth and elevation. The cross-sectional view and lengths of the design are given in Figure 7.

The feed antenna, circular waveguides, and septum polarizers are made of aluminum. The elements are connected with bolts, and sealing elements are used between them. The three-dimensional radiation pattern of the X band feed antenna and its assemblies at 8.25 GHz is shown in Figure 8. The gain of the antenna system is 19.4 dBi.

3. Assembly of Reflector Antenna with the X Band Feed Antenna

The ground stations require high-gain antennas to achieve high-gain levels for tracking LEO satellites. Thus, the developed X band feed antenna is integrated with a Cassegrain-type reflector antenna to attain high gain levels. Cassegrain reflector antennas are referred to as dual reflector antennas. The Cassegrain-type reflector structure is shown in Figure 9.

The point indicated by f_2 in Figure 9 shows the focal points of the main parabolic reflector and the hyperbolic subreflector. The focal points of both structures are placed so that they overlap. The point indicated by f_2 is the virtual focal point of the hyperbolic subreflector. The waves coming from the virtual focal point (f_2) onto the hyperbolic subreflector travel in the direction of the real focal point of the hyperbolic reflector (shown as dashed lines in Figure 9) reach the main parabolic reflector. The focal point f_2 is also the focal point of the main parabolic reflector, and for the main parabolic reflector, all waves coming from the focal point travel in a straight line. Therefore, the waves from f_2 are reflected once from both

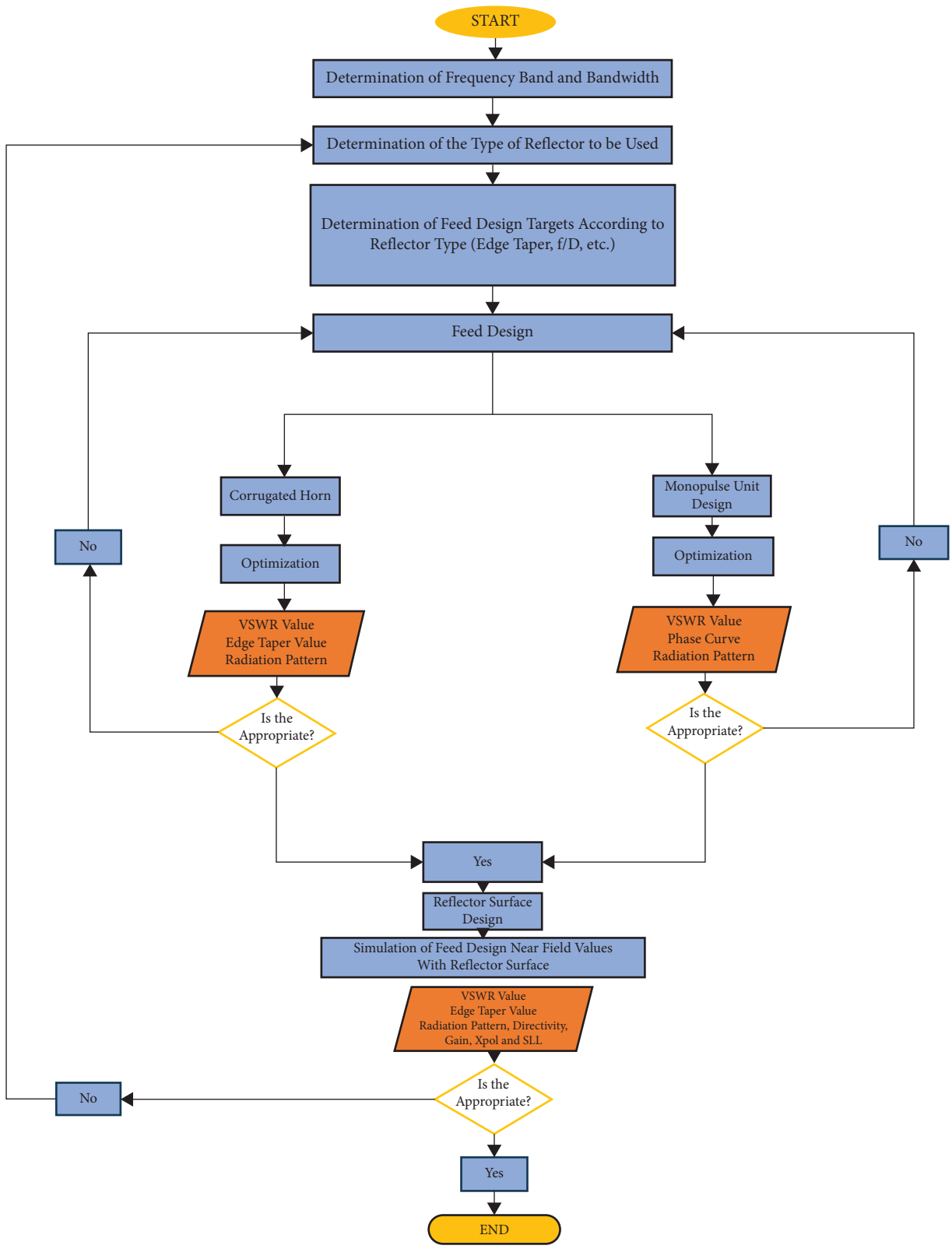

Figure 12: Flowchart of the proposed antenna design.

reflectors and propagate as plane waves. The developed X band feed antenna is placed at the focal point f_2 in the Cassegrain structure [17].

The parameters of sigma and focal point are considered when integrating the X band feed antenna onto the Cassegrain reflector. These parameters play a crucial role in the design and

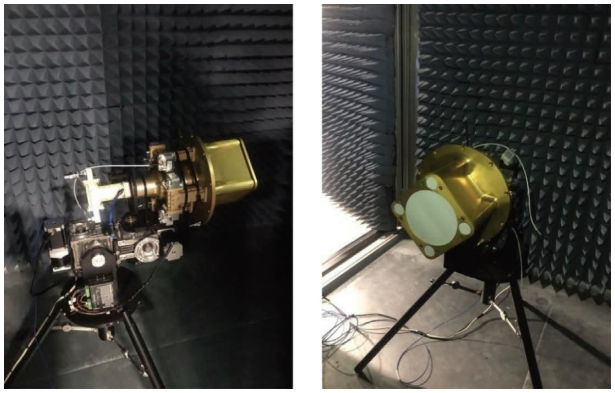

Figure 13: The measurement setup of the feed antenna.

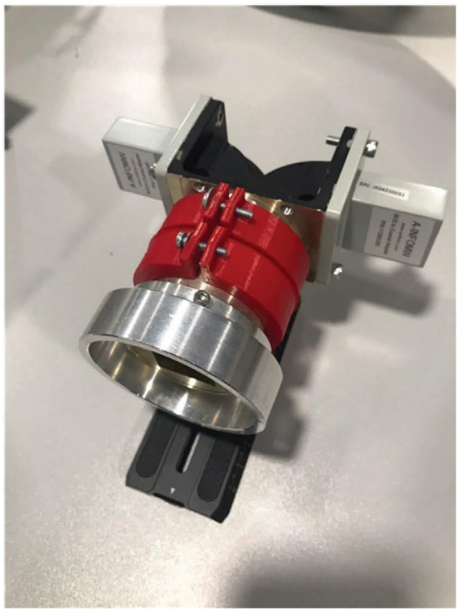

Figure 14: The fabricated reference antenna.

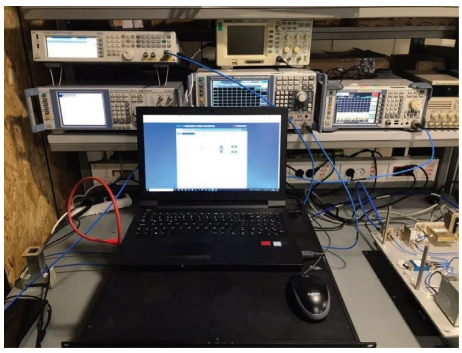

Figure 15: The control panel of the measurement.

production of reflector antennas, as they affect performance characteristics such as focusing capability and gain. A higher focal point and lower sigma value result in better performance and sensitivity. After the feed antenna system is placed on the focus of the 7.3 m Cassegrain reflector antenna, the difference model is calculated for the RHCP ports; the LHCP ports are the same as the RHCP ports. Figure 10 shows the feed antenna placed on the Cassegrain reflector antenna.

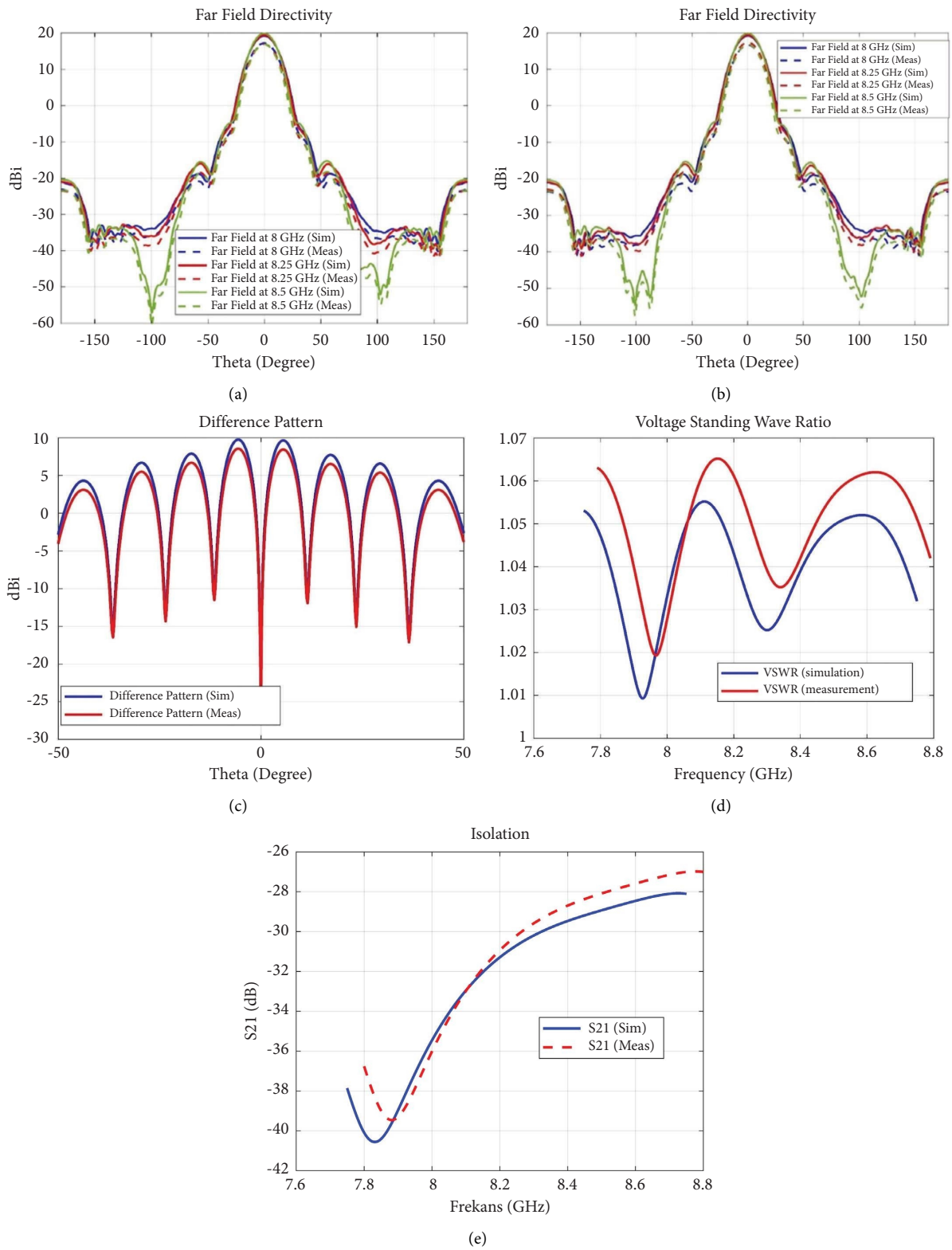

Figure 16: (a) Measurement and simulation results of the radiation pattern of the system at 8 GHz, 8.25 GHz, and 8.5 GHz for phi = 0°, (b) measurement and simulation results of the radiation pattern of the system at 8 GHz, 8.25 GHz and 8.5 for phi = 90°, (c) measurement and simulation of the difference pattern, (d) measurement and simulation results of VSWR the feed antenna, and (e) isolation of the linear ports of the septum polarize.

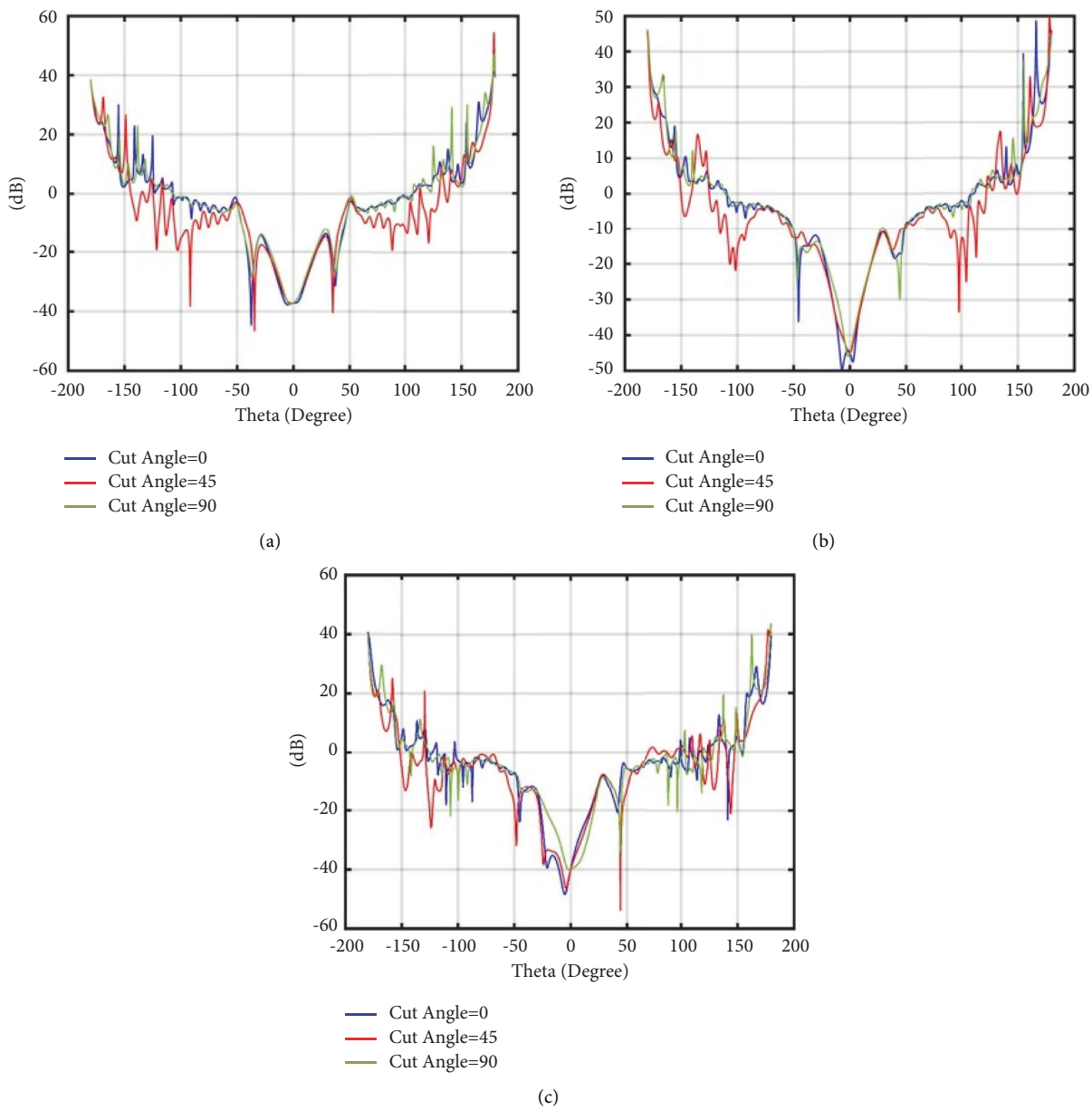

Figure 17: Measurement results of the crosspolarization of the feed antenna, (a) at 8 GHz, (b) at 8.25 GHz, and (c) at 8.5 GHz.

The system's gain is 55.3 dBi when the feed antenna system is placed on the focus of a 7.3 m Cassegrain reflector antenna. To maximize the secondary gain, the secondary sum and difference models are optimized for the given reflector and subreflector profile. The simulated secondary sum and difference pattern are shown in Figure 11.

When the antenna diameter is determined based on the required data rate for communication, the link budget is calculated as the G/T value. The progression of this design is illustrated in the flowchart shown in Figure 12.

The sum pattern fulfills the gain requirement, while the difference pattern provides the required depth and slope. The difference pattern has no distortion (Figure 11). Although the difference pattern provides a broader tracking pointing accuracy, reliable tracking is achieved by operating the system in the main lobe of the sum beam. This is achieved by providing appropriate threshold-level adjustments for tracking errors at the tracking receiver.

4. Experimental Setup

The real-time implementation of the X band feed antenna is shown in Figure 6. The fabricated version of the feed antenna is given in Figure 13.

RF measurements of the X band feed antenna were performed in an anechoic chamber. The measurements were tested at 8 GHz, 8.25 GHz, and 8.5 GHz frequencies. The X band feed antenna was placed on a motion pedestal in the anechoic chamber test. On the opposite side of the pedestal, a reference antenna with a known gain, frequency range, cross-polarization value, and input reflection value was placed in a line of sight (Figure 14). It was noted that the

Figure 18: 7.3 m Cassegrain reflector antenna.

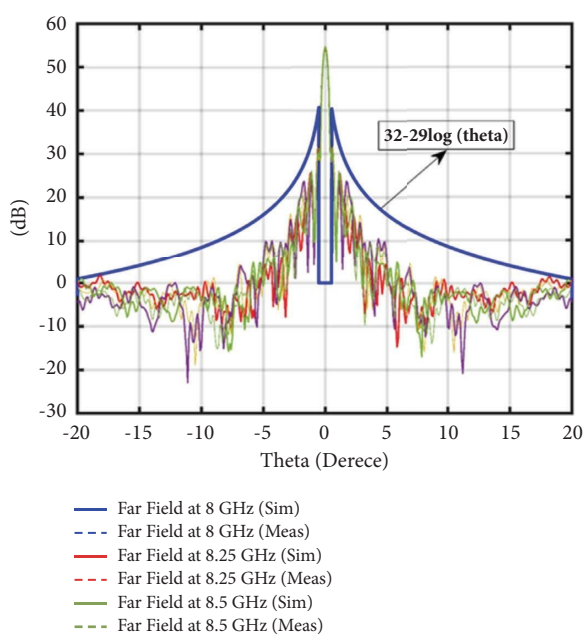

Figure 19: Measurement and simulation results of the pattern of the reflector antenna at 8 GHz, 8.25 GHz, and 8.5 GHz.

reference antenna had the same polarization as the proposed antenna.

The X band feed antenna was moved in azimuth and elevated on the movement pedestal. Patterns were realized with the spectrum analyzer (Figure 15).

The radiation patterns of the X band feed antenna are given in Figures 16(a) and 16(b). The simulation and measurement results were observed to match, and the gain patterns of the X band feed antenna were measured as 19.4 dBi.

The measurement results of the difference pattern shown in Figure 16(c) for the X band feed antenna also matched the simulation results. The null level at 0 degrees and the consistent progression of the pattern along the theta angle was critical. The measurement results supported these observations.

The desired VSWR value for the X band feed antenna was below 1.2. The VSWR value was below 1.06. A VSWR value close to 1 improved the matching performance,

Table 2: Comparison of monopulse feed antennas.

Ref	Monopulse feed	Single/Dual	Gain (dBi)	Efficiency	Polarization	Crosspolarization (dB)
[13]	No	Single band 14.5–15.35 GHz Dual band	49.3/56	56/61.5	Dual	N.A.
[22]	No	*S*-band (3.38–3.92 GHz) Ka-band (24.9–40 GHz) Dual band	13.7/32.1	42/47	Single	N.A
[19]	Yes	*S*-band (2–2.3 GHz) *X* band (7.7–8.5 GHz)	55.1/43.1	78/69	Dual	30
[20]	Yes	Single band 7.7–8.5 GHz Dual band	15.3	N.A.	Dual	25
[21]	Yes	*X* band (7.7–8.5 GHz) Ka band (25.5 GHz-27 GHz)	20.53	N.A.	Dual	22.5
This work	Yes	Single band X band (8–8.5 GHz)	54.97@8200 MHz	79.93	Dual	35

transmission efficiency, communication quality, and overall system performance (Figure 16(d)).

The crosspolarization level for the *X* band feed antenna was above 30 dB, as observed in both the simulation and measurement results. A high crosspolarization antenna could effectively handle both horizontal and vertical polarizations. The measurement results confirmed that this requirement was met (Figure 17).

The port isolation value was above 28 dB in Figure 16(e). The measurement and simulation values were similar.

High port isolation prevented signals from one port from interfering with signals from other ports. This isolation provides advantages such as interference reduction, signal clarity, accurate measurements, and system reliability. These features contributed to improved antenna system performance and stable communication.

5. Results

The *X* band feed antenna was placed on the reflector antenna with a diameter of 7.3 m, as shown in Figure 18.

The gain of the sum signal was 54.97 dBi, the communication signal (Figure 19). The antenna efficiency was approximately 79.93%. Additionally, the null level of the tracking signal had a smooth pattern at 0 (Figure 19). It is desirable to have these patterns to be smooth for good satellite tracking.

G/T was measured from the terrestrial sources from Sun Methods [18], 32 dB/K. A low-noise amplifier (43 K noise temperature) was integrated with the feed to minimize noise. Satellite autotracking was established by realizing a single-band multielement monopulse tracking.

6. Conclusion

An *X* band feed antenna is designed for the LEO satellite ground station. *X* band feed antenna system offers a high G/T ratio (32 dB/K for the *X* band) and a low crosspolarization response and low side lobe level.

A ground station design was implemented by integrating an *X* band feed antenna with a 7.3 m Cassegrain-type reflector. According to the simulation results, the gain values at 8 GHz, 8.25 GHz, and 8.5 GHz frequencies were measured at above 55.0 dBi, the VSWR value was 1.1, the side lobe level was below −24 dB, the crosspolarization value was below −35 dB, and the port isolation value was below −29 dB. The measurement results showed a gain value of 54.97 dB at 8.2 GHz frequency, VSWR value of 1.15, side lobe level above −24 dB, crosspolarization value above −30 dB, and port isolation value above −28 dB. G/T is a satellite system's figure of merit (FOM). G is the received antenna gain. T is the system noise temperature [3]. The figure of merit, the G/T value for the ground station system, was measured above 32 dB/K. A high G/T value is an essential parameter for ground stations because it provides significant advantages such as extending the transmission distance, achieving sensitivity even at low power levels, reducing noise, and improving data quality to have reliable and high-performance communication systems.

Considering our target requirements, the results indicate that all performance outputs match our target ones. The effectiveness of the ground station antenna was found to be 79.93%. Compared to the 7.3 m reflector antenna diameter, such a high efficiency was attained. The suggested feed antenna is highly efficient, small, cost-effective, adheres to the overall design style, and is ideal for use as a ground station reflector feeder antenna that fulfils strict industry standards.

In comparison to [7] in this study, our antenna demonstrates better performance in terms of efficiency, especially when considering the antenna diameter. Additionally, in the presented design, the crosspolarization isolation value is above 35 dB in Figure 17, and the side lobe level exceeds 24 dB in Figure 19, resulting in superior overall performance. This directly influences the system G/T value. The monopulse tracking block diagram provided in Figure 9 differs from [7], showcasing a distinct tracking architecture. In the presented structure, the TE11 mode from both azimuth and elevation is initially combined and then fed into a 180° hybrid coupler and subsequently into a 90° hybrid coupler. This configuration allows the system to track in both RHCP and LHCP, creating a versatile tracking system.

Considering our target requirements (Table 1), the gain of the proposed study is better than other comparable works' gain, except for [19], which has lower efficiency and crosspolarization than the proposed study. Compared to

similar designs [20, 21], the proposed design improves the gain, efficiency, and crosspolarization.

The comparison of feed antennas with their features which are single/dual, gain, efficiency, polarization, and crosspolarization is presented in Table 2. Various research studies for the single-band operation have previously been made to find the best feed for monopulse tracking [13] Out of available monopulse feed configurations, four elements [19] and multimode feed [20, 21] have been used depending on the application, system specification, and cost-effectiveness.

Data Availability

The data used to support the findings of this study are available from the corresponding author upon reasonable request.

Conflicts of Interest

The authors declare that there are no conflicts of interest regarding the publication of this paper.

References

[1] G. Hawkins, D. Edwards, and J. McGeehan, "Tracking systems for satellite communications," in *IEE Proceedings F (Communications, Radar and Signal Processing)*, vol. 135, pp. 393–407, IET, England, UK, November 1988.

[2] I. Sisman and T. H. Ergin, "Monopulse chaparral choke antenna design and implementation for satellite communication systems," in *2023 IEEE- APS Topical Conference on Antennas and Prop- agation in Wireless Communications (APWC)*, p. 179, IEEE, Venice, Italy, October 2023.

[3] S. A. Elgamel and J. Soraghan, "Enhanced monopulse tracking radar using optimum fractional Fourier transform," *IET Radar, Sonar and Navigation*, vol. 5, no. 1, pp. 74–82, 2011.

[4] P. K. Willett, W. D. Blair, and Y. Bar-Shalom, "Correlation between horizontal and vertical monopulse measurements," *IEEE Transactions on Aerospace and Electronic Systems*, vol. 39, no. 2, pp. 533–549, 2003.

[5] M. A. Latifzade, M. R. Arvan, and H. Mohseni Armaki, "Monopulse antenna-pointing system modelling and simulation," *IET Radar, Sonar and Navigation*, vol. 13, no. 4, pp. 646–652, 2019.

[6] S. S. Roy, C. Saha, T. Nagasekhar et al., "Design of a compact multielement monopulse feed for ground-station satellite tracking applica- tions," *IEEE Antennas and Wireless Propagation Letters*, vol. 18, no. 9, pp. 1721–1725, 2019.

[7] H. R. Heidari, P. Rezaei, S. Kiani, and M. Taher- inezhad, "A monopulse array antenna based on siw with circular polarization for using in tracking systems," *AEU-International Journal of Electronics and Communications*, vol. 162, Article ID 154563, 2023.

[8] H. Bartlett, E. Smith, and T. Gutwein, "Five-horn Cassegrain feed with sidelobe crossover," in *1977 Antennas and Propagation Society International Symposium*, vol. 15, pp. 332–335, IEEE, Stanford, CA, USA, June 1977.

[9] H. Bartlett, "A broadband five-horn Cassegrain feed," in *1978 Antennas and Propagation Society International Symposium*, pp. 350–354, London, UK, November 1978.

[10] Y. H. Choung, K. R. Goudey, and L. G. Bryans, "Theory and design of a Ku-band TE/sub-21/- mode coupler," *IEEE Transactions on Microwave Theory and Techniques*, vol. 30, no. 11, pp. 1862–1866, 1982.

[11] N. Rezazadeh and L. Shafai, "Ultrawideband monopulse antenna with application as a reflector feed," *IET Microwaves, Antennas and Propagation*, vol. 10, no. 4, pp. 393–400, 2016.

[12] S. Kiani, P. Rezaei, and M. Fakhr, "A cpw-fed wearable antenna at ism band for biomedical and wban applications," *Wireless Networks*, vol. 27, no. 1, pp. 735–745, 2021.

[13] S. M. Sherman and D. K. Barton, *Monopulse Principles and Techniques*, Artech House, Norwood, MA, USA, 2011.

[14] C. Kumar, V. Srinivasan, V. Lakshmeesha, and S. Pal, "Novel dual circularly polarized radiating element for spherical phased-array application," *IEEE Antennas and Wireless Propagation Letters*, vol. 8, pp. 826–829, 2009.

[15] E. S. Solvers and C. Compatibility, "CST Studio suite," 2020, https://www.3ds.com/ko/products-services/simulia/products/cst-studio-suite/solvers/.

[16] R. E. Collin, *Foundations for Microwave Engineering*, John Wiley & Sons, Hoboken, NJ, USA, 2007.

[17] S. K. Sharma, S. Rao, and L. Shafai, *Handbook of Reflector Antennas and Feed Systems Volume I: Theory and Design of Reflectors*, Artech House, Norwood, MA, USA, 2013.

[18] W. C. Daywitt, "On 10-60 ghz g/t measurements using the sun as a source: a preliminary study," Report, National Bureau of Standards, Gaithersburg, MD, USA, 1986.

[19] S. S. Roy, T. Nagasekhar, C. Saha et al., "Dual band (SX) ground station antenna for low earth orbit (LEO) satellite tracking application," *IEEE Access*, vol. 10, pp. 80910–80917, 2022.

[20] F. Dubrovka, S. Martunyuk, R. Dubrovka et al., "Circularly polarised x-band h11-and h21-modes antenna feed for monopulse autotracking ground station," in *2020 IEEE Ukrainian Microwave Week (UkrMW)*, pp. 196–202, IEEE, Kharkiv, Ukraine, September 2020.

[21] A. T. Mothe, C. Saha, and S. S. Roy, "Dual band (x-ka) smooth-wall multimode monopulse feed for leo satellite tracking," in *2021 IEEE Indian Con- ference on Antennas and Propagation (InCAP)*, pp. 953–956, IEEE, Rajasthan, India, December 2021.

[22] S. Rao, L. Shafai, and S. K. Sharma, *Handbook of Reflector Antennas and Feed Systems Volume III: Applications of Reflectors*, Artech House, Norwood, MA, USA, 2013.